Journal of Inorganic and Organometallic Polymers and Materials (2021) 31:683–694
https://doi.org/10.1007/s10904-020-01697-1

Self-healing Polyurethane Elastomer Based on Molecular Design: Combination of Reversible Hydrogen Bonds and High Segment Mobility

Zhaopeng Liang[1] · Dongao Huang[1] · Lei Zhao[1] · Yijing Nie[1] · Zhiping Zhou[1] · Tongfan Hao[2] · Songjun Li[1]

Received: 29 June 2020 / Accepted: 31 July 2020 / Published online: 8 August 2020

Abstract
Polyurethane (PU) belongs to a class of special polymeric materials with hydrogen bonds, which has the potential for self-healing ability. In the present work, by introducing polypropylene glycol (PPG) blocks with high segment mobility and different block lengths on the ends of PU chains, the PUs with adjustable self-healing ability were successfully obtained. The self-healing ability of the PUs firstly increases with the increase of the PPG block lengths, but then decreases. This phenomenon can be attributed to the combined effects of the density of hydrogen bonds and the mobility of PPG segments. At first, the increase of the PPG block length leads to the improvement of mobility of PU chains, which is beneficial for the enhancement of the self-healing. However, the further increase of the PPG block length results in the reduction in the hydrogen bond density, finally leading to the decrease of the self-healing ability of the PUs.

Keywords Polyurethane · Self-healing · High segment mobility · Hydrogen bonds

1 Introduction

Nowadays, the shortage of non-renewable resources is becoming increasingly serious, which to some extent restricts the economic and social developments. In addition, the waste of resources and the environmental pollution caused by the damage and scrap of materials are becoming more and more serious. Therefore, vigorously developing self-healing polymer materials to extend the service life of materials is of great significance not only to cope with the current resource crisis and environmental problems, but also to promote sustainable economic and social developments [1–8].

The preparation of intrinsic self-healing polymer materials is one of the hotspots in the field of polymer science and engineering [1, 3–8], which refers to one kind of polymer materials that can self-repair without any additional energy and force, if the corresponding polymer is damaged. There are two categories of intrinsic self-healing polymer materials, including polymer with reversible covalent bonds [3] and that with reversible non-covalent bonds [4].

Rubber or elastomer belongs to an important class of polymer materials, which has been widely used in our daily life [9–15]. As is well known, polyurethane (PU) has a wide range of applications and is considered as one of polymer materials that cannot be separated from the modern industrial production and human life [16–18]. Then, many efforts have been devoted to the design and preparation of self-healing PU by introducing reversible covalent bonds [19, 20] or reversible non-covalent bonds, such as hydrogen bonds [21, 22], ionic interactions [23] and metal–ligand coordinations [24]. In general, the development of the self-healing PU with reversible covalent bonds depends on the special chemical reactions, such as the reversible Diels–Alder reaction [25] and the disulfide exchange reaction [19]. However, the corresponding synthesis is somewhat complicated, and in some conditions the corresponding chemicals are toxic (for instance, disulfide). Then, the development of the

✉ Yijing Nie
nieyijing@ujs.edu.cn

✉ Songjun Li
lsjchem@ujs.edu.cn

[1] Research School of Polymeric Materials, School of Materials Science and Engineering, Jiangsu University, Zhenjiang, China

[2] Institute of Green Chemistry and Chemical Technology, Jiangsu University, Zhenjiang, China

self-healing PU with the reversible non-covalent bonds seems to have certain advantages [6, 7, 21–24]. For instance, Wang et al. introduced multiple metal–ligand coordination in their self-healing PU, and demonstrated that the corresponding physical cross-linking due to the multiple metal–ligand coordination can be fully reformed [24]. Incorporation of multiple hydrogen bonding was also proven to be an effective method to improve the self-repairing ability of PU [21, 22]. In addition, ionic interaction can play an important role in the construction of a reversible network for the rapid self-healing in alginate-based ionic PU [23]. More interestingly, Zhang et al. reported that the coexistence of the different reversible non-covalent bonds, that is, dimethylglyoxime-urethane (DOU) bonds, Cu-DOU coordination bonds and hydrogen bonds, can endow PU with mechanical robustness and self-healing efficiency together [26].

It should be noted that PU itself has some unique advantage for the design based on the reversible hydrogen bonds due to its special chemical structure. PU chains are composed of two kinds of chain sections: soft blocks composed of polyether polyol or polyester polyol and hard blocks consisting of the diisocyanate and short chain extenders [16]. Luckily, intermolecular hydrogen bonds can form between neighboring urethane groups [16], and thus can contribute to the ability of the self-healing. Besides, soft blocks have a strong mobility and thus can diffuse easily through cracks, which is another prerequisite for achieving good self-healing behaviors [27, 28]. Apparently, the distribution of intermolecular hydrogen bonds and the mobility of soft segments should depend on the chemical structures of both hard and soft segments and the length of soft segments in PU chains. In other words, the self-healing behaviors of PU are closely dependent on its chain structure. Wu et al. introduced polytetramethylene ether glycol (PTMEG) blocks into main chains as soft segments during the synthesis of PU, and thus the corresponding chain mobility at room temperature is improved, resulting in excellent self-healing behaviors [29]. Lai et al. proved that the reinforcement effect of hard segments in PU is due to physical crosslinking [30]. However, the presence of too many hard segments will reduce the fluidity of chain segments, which is not conducive to the self-healing process [30]. However, the influence of chain structure on the self-healing of PU is received enough attention. In order to precisely control the self-repairing ability of PU or prepare new PU with superior self-healing ability by designing its chemical structure, the relationship between the self-repairing behaviors and the chain structure of PU should be first understood.

In the present work, a new kind of PU chains containing soft blocks with different block lengths in their two ends was synthesized. These soft blocks existing in the ends of PU chains have relatively strong mobility, which is beneficial for the chain diffusion around damage areas and the self-healing process. In addition, the existence of hydrogen bonds forming between amine in the urethane groups and carbonyl groups can further provide guarantee for the efficient healing of fractures in these PU materials.

2 Experimental Section

2.1 Materials

Isophorone diisocyanate (IPDI) was provided by National Pharmaceutical Reagent Company. Polycarbonate glycol (PCDL-1000 and Mn = 1000) was supplied by Jining Hua Kai Resin Co., Ltd. Polypropylene glycol (PPG) with different Mn, that is, 400, 600, 1000 and 2000 (PPG-400, PPG-600, PPG-1000 and PPG-2000) was also bought from Jining Hua Kai Resin Co., Ltd. In addition, some other chemicals, including 1, 4-butanediol (BDO), dibutyltin dilaurate (DBTDL) and *N*,*N*-Dimethylacetamide (DMAC) were all obtained from Sinopharm Chemical Reagent Co., Ltd.

2.2 Synthesis of PU

Herein, we first used IPDI, PCDL-1000 and the chain extender BDO to synthesize isocyanate-terminated linear polyurethane. Then, in order to obtain the PCDL-terminated polyurethane (PU-0), PCDL-1000 was further added (the reaction mechanism can be seen in Scheme 1). In addition, to synthesize the PPG-terminated polyurethane, PPG with different molecular weights (400, 600, 1000 and 2000, respectively) was used for the further reaction instead of PCDL-1000, and thus a series of linear polyurethanes (PU-400, PU-600, PU-1000 and PU-2000, respectively) are synthesized (the reaction mechanism can be seen in Scheme 2). The detailed experimental procedure can be seen as follows.

Firstly, 33.34 g IPDI, 100 g PCDL and 20 g DMAC were added into the flask, stirred at a constant speed and then heated up to 80 °C. After keeping for 2 h, the system was cooled down to 60 °C. Then, 3.38 g BDO and 30 g DMAC were further added, and the temperature was increased to 80 °C. The system was maintained at 90 °C for 1 h, and then 1 drop of DBTDL catalyst was added. Subsequently, the system was further stirred at a constant speed for 1 h. After that, we titrated to measure the content of -NCO groups once every 15 min until the theoretical value was reached. Furthermore, after the system was cooled below 60 °C, 20 g PCDL-1000/8 g PPG-400/12 g PPG-600/20 g PPG-1000/40 g PPG-2000 and 20 g DMAC were added. The temperature was raised to 85 °C, and the system was stirred at a constant speed for 2 h. Finally, the synthesized PU samples were poured into polytetrafluoroethylene mold and dried at 80 °C in a blast oven for 2 days.

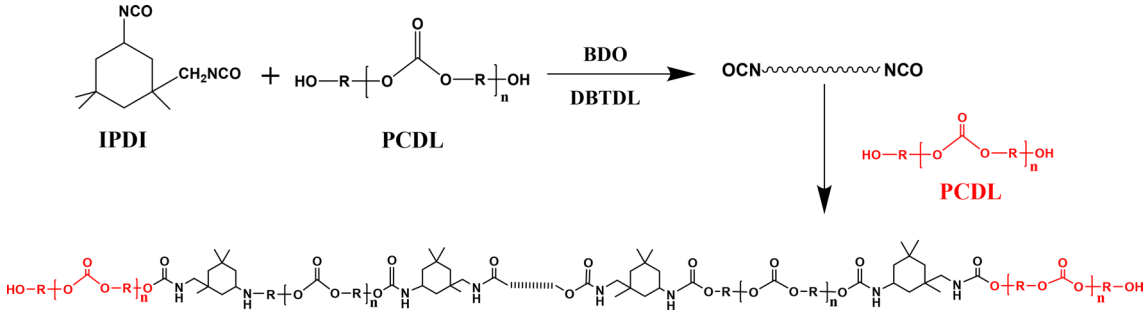

Scheme 1 Basic steps of the synthesis of PU-0 with PCDL end blocks

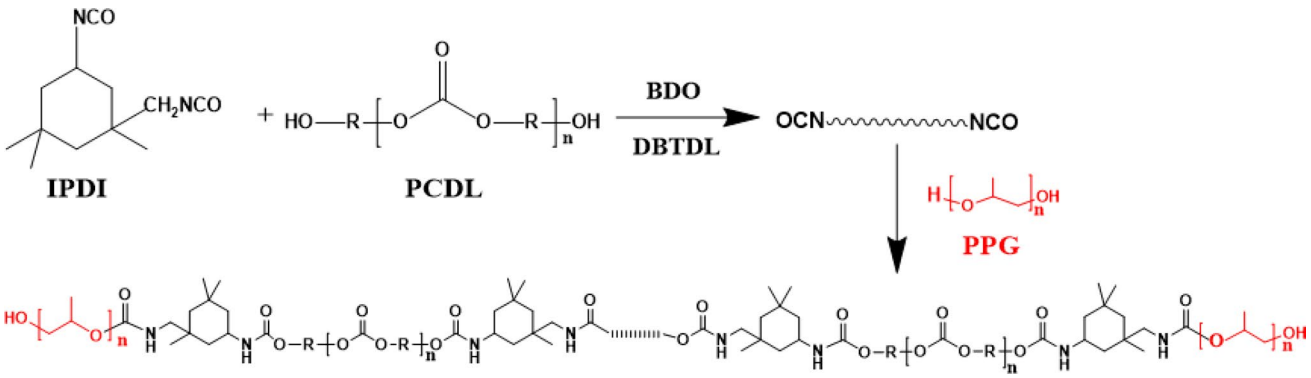

Scheme 2 Basic steps of the synthesis of PU with PPG end blocks

2.3 Characterization

2.3.1 Gel Permeation Chromatography (GPC)

The molecular weight of the PU samples was tested by using GPC on a Waters 1515 device. DMF was used as the flow phase with a flow rate 1.5 mL/min and monodisperse PEO was used as standard with a column temperature of 40 °C.

2.3.2 Fourier Transform Infrared Spectroscopy (FTIR)

FTIR spectra of different PU samples were measured and recorded at room temperature (about 25 °C) on Nicolet Nexus 470 Type Fourier Transform Infrared Spectrometer. In addition, in order to demonstrate the presence of hydrogen bonds, FTIR spectra of these PU samples under high temperature (85 °C) were also measured. The scanning resolution was 4 cm^{-1}, and the scanning times were 32. A series of samples were made into sheet samples and tested in ATR mode of the infrared spectrometer.

2.3.3 ^{1}H-NMR

^{1}H-NMR spectra of the different PU samples were measured by Bruker avanceiii-400 nuclear magnetic resonance spectrometer (600 MHz), and deuterium chloroform was used as solvent.

2.4 Self-healing Test

2.4.1 Weight Hanging Experiments of Healed Samples

The PU-600 sample was first cut into two pieces and then healed at 50 °C for 2 h. After that, two different weights of 850 g and 2225 g were hanged on the healed sample, respectively.

2.4.2 Morphology Observation of Self-healing Process

The self-healing process of the PU-600 sample was observed by optical microscopy. The sample was cut into two parts by a clean blade, and then the two separated parts were contacted immediately after the cutting. Then, XSP-002 optical microscope was used to detect the changes in the fracture surface of the healed sample.

2.4.3 Mechanical Tests of Self-healed Specimens

We carried out tensile tests of each self-healed sample before and after self-healing process under different healing

temperatures or healing times. The corresponding tensile tests were carried out on the AGS-X50kN universal tensile machine at the rate of 100 mm/min, and five parallel experiments were carried out for each sample under each condition.

2.4.4 Two Consecutive Tensile Tests

In order to reveal the effect of hydrogen bonds on the recovery of mechanical properties, two consecutive tensile tests were carried out for these PU samples using the AGS-X50kN universal tensile machine. The PU sample was first stretched to a predetermined strain (12%). Then, the stretching process stopped and the sample retracted. After a period of time (20 min and 12 h, respectively), the same sample was stretched again to the predetermined strain (12%).

3 Results and Discussion

The molecular weight data of a series of the PUs synthesized are shown in Table 1. The results reflected from the data are in line with expectations, that is, the molecular weight of the PU-400 is the smallest, that of the PU-2000 is the largest, and that of the PU-0 and the PU-1000 are roughly similar. Considering the errors due to the synthesis process, the gaps between these molecular weight data of the PU samples are basically consistent with expectations.

In order to confirm that the PUs containing soft PPG end blocks with different block lengths have been successfully synthesized, the FTIR spectra of the different PU samples were recorded, as shown in Fig. 1. It can be seen that all of the spectra exhibit the absorption peaks around 3335 cm^{-1}, 2934 cm^{-1}, 1737 cm^{-1}, 1250 cm^{-1} and 1530 cm^{-1}, corresponding to the stretching vibrations of –OH or –NH–, $–CH_2–$ or $–CH_3$, C=O and C–O in carbonate and urethane groups and the bending vibration of –NH– [31–33], demonstrating the existence of hydroxyl groups, urethane groups, methylene and carbonate groups in PU chains (that is, the PU-0 containing PCDL end blocks has been successfully synthesized). In addition, the FTIR spectra of the PU terminated by PPG, including the PU-400, the PU-600, the PU-1000 and the PU-2000, show a new absorption peaks at 1112 cm^{-1}, attributed to the appearance of the stretching vibration of ether oxygen bond [34, 35], and the intensity increases with increasing the length of PPG chain sections, demonstrating that the PU samples terminated by PPG with different block lengths have been successfully obtained.

Table 1 The molecular weight date of the different PU samples

GPC	PU-0	PU-400	PU-600	PU-1000	PU-2000
Mn	78,440	77,035	77,468	78,227	80,376

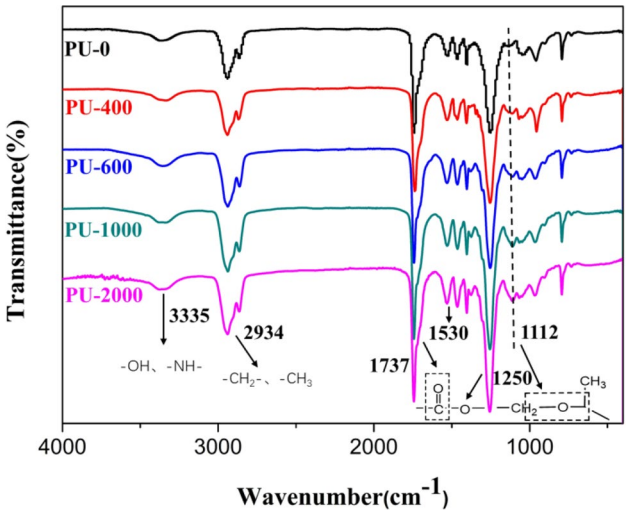

Fig. 1 FTIR spectra of different PU samples, including PU-0, PU-400, PU-600, PU-1000 and PU-2000

In addition, ^{1}H-NMR spectra were also measured to confirm the successful synthesis of the PU-0 and the PU terminated by PPG. Figure 2 depicts the ^{1}H-NMR spectra of the PU-0 and the PU-600 samples. It can be clearly seen that the peaks appear at 4.13 ppm (e, $–OCOOC\mathbf{H_2}CH_2–$), 1.70 ppm (f, $–OCOOCH_2C\mathbf{H_2}CH_2–$) and 1.42 ppm (g, $–OCOOCH_2CH_2C\mathbf{H_2}CH_2–$) in the ^{1}H-NMR spectrum of the PU-0 sample [36], which represent the characteristic signal peaks of the soft PCDL segments. One can also clearly see that the e′ peak appears at 3.67 ppm, which represents the signal peak ($–CH_2C\mathbf{H_2}OH$) of the methylene adjacent to the inner side of the end hydroxyl when PCDL is used as the chain ends [37]. In short, the above findings can prove that

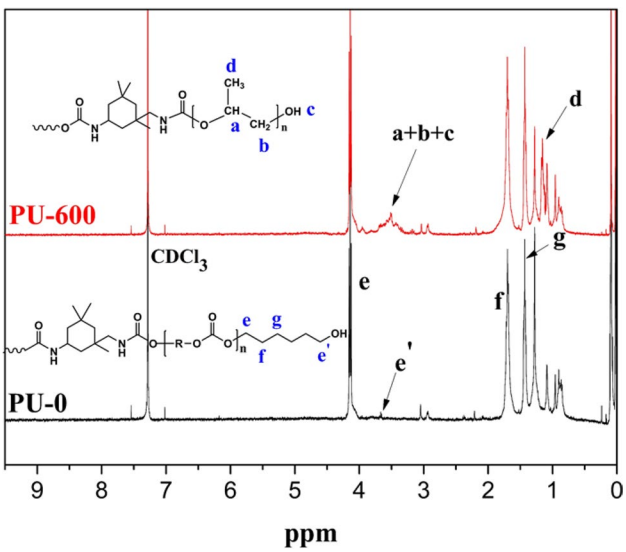

Fig. 2 ^{1}H-NMR spectra of PU-0 and PU-600

Table 2 The average tensile strengths for different PU samples

	PU-0	PU-400	PU-600	PU-1000	PU-2000
Tensile strength (MPa)	33.6	26.8	20.1	16.0	16.3

PCDL segments were successfully introduced as soft segments and chain ends. Similarly, there are three peaks (that is, e, f and g peaks) in the ^{1}H-NMR spectrum of the PU-600 sample, demonstrating that the PCDL segments exist in the PU chains. In addition, there are a series of broad peaks at 3.27–3.76 ppm, representing the signal peaks of methylene (a, –OC**H**(CH_3)CH_2–), methylene (b, –OCH(CH_3)C**H$_2$**–), hydroxyl (c, –CH_2O**H**), and a strong methyl signal peak (d, –OCH(C**H$_3$**)CH_2–) at 1.14 ppm [38]. The appearance of these peaks can confirm that the PPG segments were introduced as the chain ends of the PU chains.

Furthermore, the mechanical properties of all the original PU samples were tested, and the corresponding values of the average tensile strength for these different PU samples were listed in Table 2. It can be observed that the PU-0 sample exhibits the highest tensile strength. In addition, the tensile strength of the PPG-terminated PUs decreases with increasing block length of PPG blocks except that of the PU-2000 sample, which displays a higher tensile strength compared with that of the PU-1000 sample. It is well known that urethane carbonyl groups and carbonyl groups in PCDL segments have stronger ability to form hydrogen bonds with urethane NH groups, compared with ether oxygen [16]. Thus, the increase of the length of the PPG blocks can lead to the decrease of the density of stronger hydrogen bonds between urethane NH groups and urethane carbonyl groups or carbonyl groups in PCDL blocks, resulting in the decrease of the tensile strength. However, on the other hand, the increase of the molecular weight of the PPG blocks can lead to the increase of the mechanical properties [39, 40]. For the PU-2000, this positive effect of the increase of molecular weight on the mechanical properties overwhelms the negative effect of the decrease of hydrogen bond density, and thus it exhibits the higher tensile strength compared with the PU-1000.

Fig. 3 **a** PU-600 sample with different weight suspending (from left to right are 850 g and 2225 g loadings, respectively), and this sample was healed at 50 °C for 2 h

Then, we further pay our attention to the self-healing behaviors of these PU samples. Firstly, in order to simply examine whether the PU examples have the self-healing ability, the weight hanging experiments of the healed PU-600 sample were carried out. As shown in Fig. 3, it can be clearly seen that the self-healed sample can successful withstand both the weights of 850 g and 2225 g, demonstrating that the PU-600 sample has a strong ability of self-healing.

In order to observe the self-healing process and the change of the fracture surfaces more clearly, the experimental observation on the morphology changes of the healed PU-600 sample were also performed, as illustrated in Fig. 4. A crack exists in the optical microscope picture of the cut sample (the leftmost panel in Fig. 4). However, as the healing time proceeds, the crack becomes more and more blurred. When the healing time reaches 60 min, even no crack can be found in the picture of the healed sample, further demonstrating that the PU-600 sample has a strong self-healing ability.

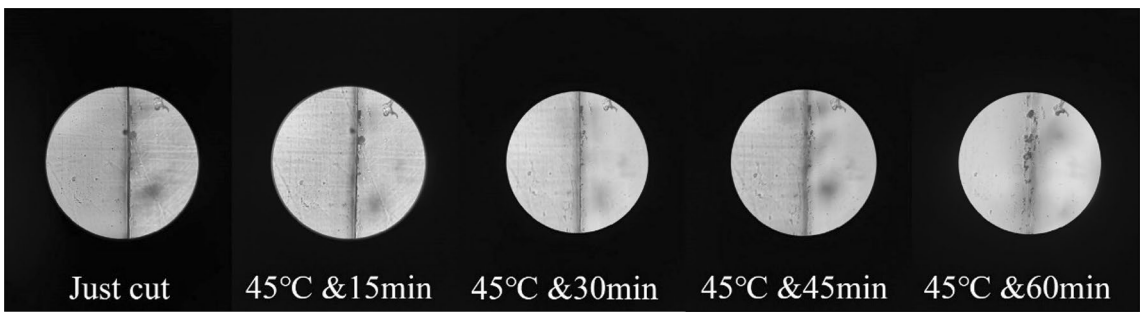

Fig. 4 Optical microscope pictures of the cut sample and the healed samples with different healing time at the magnification of × 500

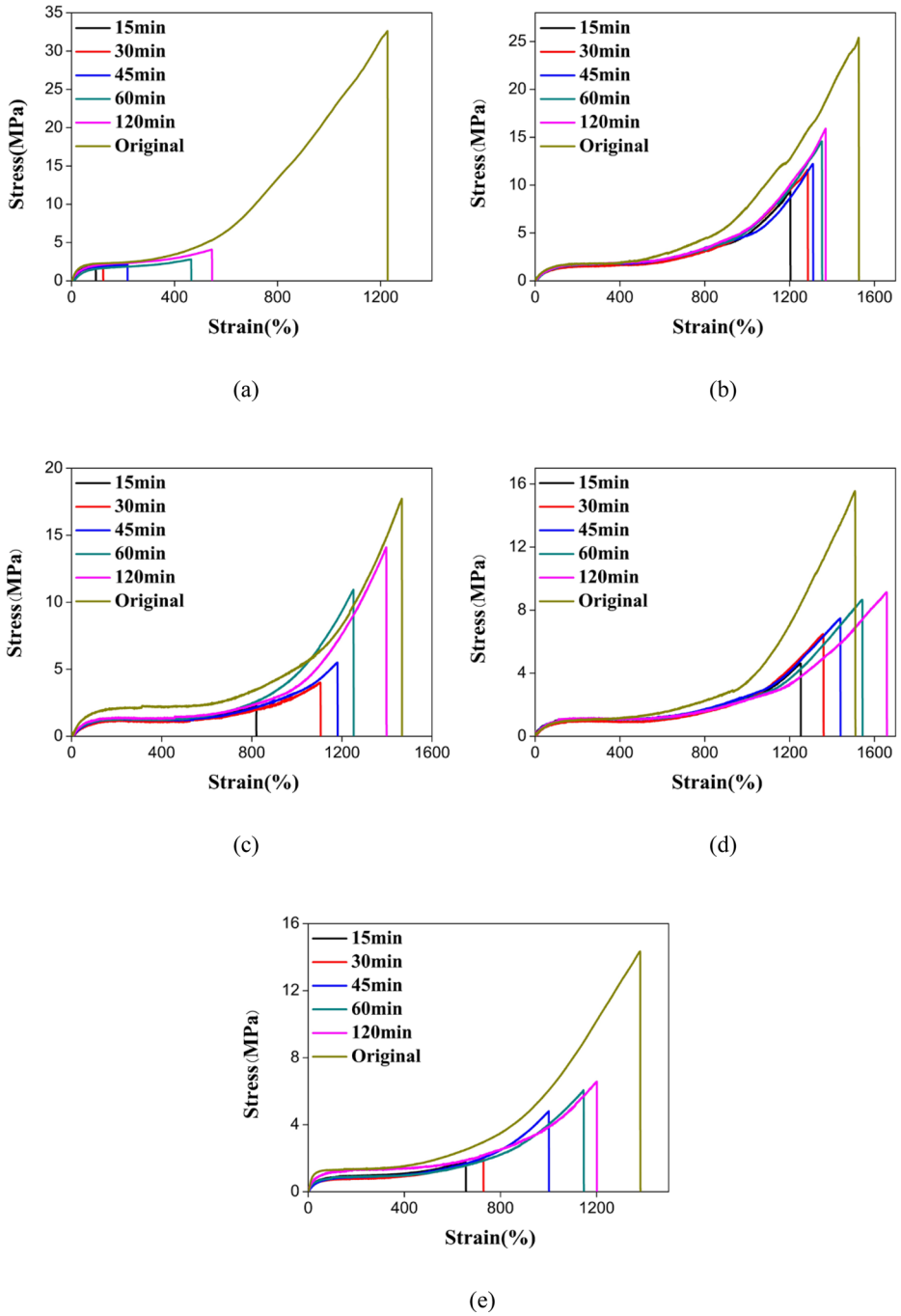

Fig. 5 Stress–strain curves of different original PU samples and these healed for different times at 45 °C, that is, **a** PU-0, **b** PU-400, **c** PU-600, **d** PU-1000 and **e** PU-2000

Table 3 The degree of the recovery of tensile strengths for the different PU samples healed for different healing times at a same temperature (45 °C)

	15 min (%)	30 min (%)	45 min (%)	60 min (%)	120 min (%)
PU-0	5.10	5.57	6.28	8.87	13.10
PU-400	36.75	45.69	48.13	57.50	62.62
PU-600	13.32	22.75	31.44	61.73	79.85
PU-1000	30.15	41.92	48.15	55.84	58.95
PU-2000	12.16	13.86	33.41	42.46	45.92

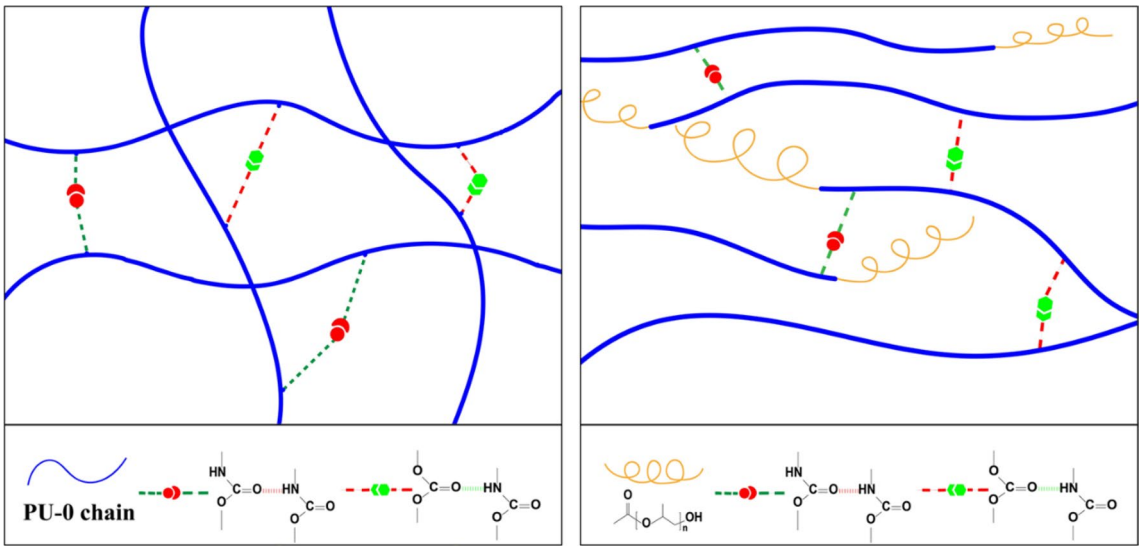

Scheme 3 Schematic model of hydrogen bonds in (left panel) PU-0 and (right panel) PU containing PPG segments

The mechanical properties were further tested to quantitatively reveal the self-healing ability of the different PU-samples. The stress–strain curves of the different original PU samples and these healed for different times at 45 °C were shown in Fig. 5. It can be observed that the original PU samples exhibit the highest tensile strength. In addition, the tensile strength of these healed samples increases with increasing healing time. Furthermore, the degree of the recovery of the tensile strengths for the different PUs was listed in Table 3 (the recovery degree of tensile strength is defined as the ratio of tensile strength of healed samples to that of original samples). For all the PU samples, the degree of the recovery of the tensile strengths increases with increasing healing time, demonstrating that prolonging the healing time is beneficial to improve the healing effect [4, 22, 28, 41]. In addition, the different PUs exhibit different self-healing behaviors. The recovery degree of tensile strength of the PU-0 is lowest among these PU samples, indicating that the presence of the flexible PPG blocks at the ends of PU chains can indeed improve the self-healing ability of the PU samples. Apparently, this improvement of the self-healing ability in these PU samples containing the PPG end blocks can be attributed to the strong mobility of the PPG segments. It has been reported that the glass transition temperature of PPG is around − 70 °C [42], which is much lower than that of PCDL (about − 40 °C) [43]. That is, PPG segments have stronger mobility than PCDL segments. Thus, the presence of PPG in the PU samples can improve the segmental mobility of the PU chains, which is beneficial for the process of self-healing process [22, 28]. Besides, as also shown in Table 3, the PU-600 has the highest degree of recovery of the tensile strength among the PU samples containing PPG blocks, suggesting that the PU-600 exhibits the strongest self-healing ability. In other words, both too short and too long PPG blocks would lead to the reduction of the self-healing ability.

In addition to segmental mobility, the presence of the reversible hydrogen bonds in the PU chains will also influence the self-healing behaviors [4, 5, 22, 41]. As is well known, the hydrogen bonds can form again through the fracture surfaces, and this process can facilitate the self-healing process. Obviously, the density of hydrogen bonds can directly affect the self-healing behaviors. In the PU-0 sample, the hydrogen bonds form between urethane carbonyl groups or carbonyl groups in PCDL segments and urethane NH groups, as illustrated in the left panel of Scheme 3. In the PU samples containing PPG end blocks, the hydrogen bonds can also form between carbonyl groups and urethane NH groups. However, no hydrogen bonds can form between the PPG segments and urethane NH groups, as shown in the right panel of Scheme 3. In this condition, the density of hydrogen bonds in the PUs containing PPG end blocks should be lower than that in the PU-0.

In other words, since it is difficult to form hydrogen bonds between –NHCOO- and PPG blocks, the increase of the length of the PPG blocks would lead to the decrease in the density of the hydrogen bonds, which would weaken the ability of the self-healing of the PU samples. In short, the presence of PPG segments results in double-edged sword effect: on one hand, the increase of the PPG length can lead to the increase of fraction of highly mobile segments, which is beneficial for the self-healing process; on the other hand,

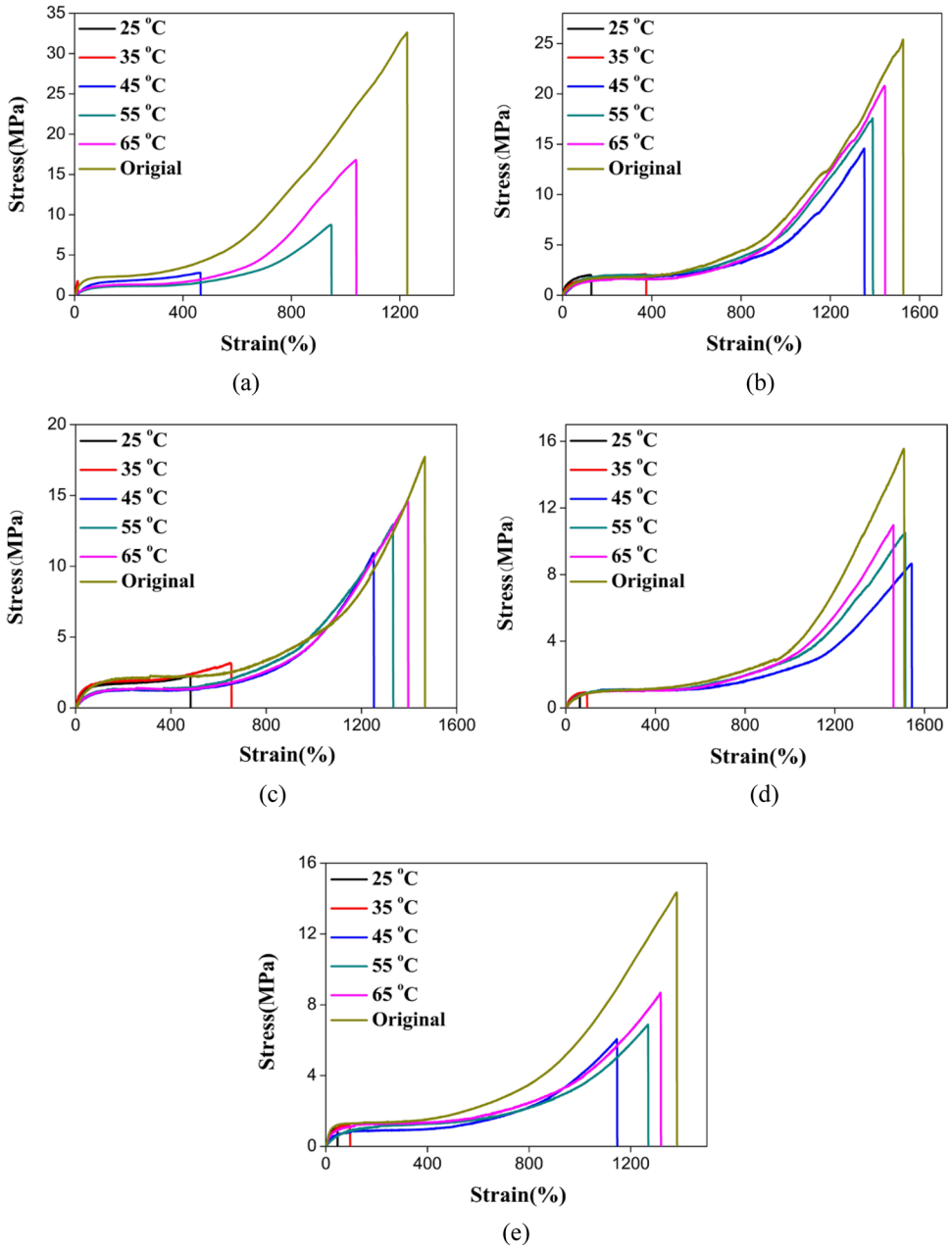

Fig. 6 Stress–strain curves of different original PU samples and these healed for different 1 h at different temperatures; **a** 25 °C, **b** 35 °C, **c** 45 °C, **d** 55 °C and **e** 65 °C

Table 4 The degree of the recovery of tensile strengths for the different PUs healed at different healing temperatures with a same healing time (1 h)

	25 °C (%)	35 °C (%)	45 °C (%)	55 °C (%)	65 °C (%)
PU-0			8.87	27.00	51.26
PU-400	7.67	8.15	57.34	68.96	81.04
PU-600	12.57	18.28	61.98	73.16	82.54
PU-1000	5.20	5.91	55.84	67.36	70.23
PU-2000	6.97	8.23	42.46	47.87	60.84

the increase of the length of the PPG blocks can also result in the decrease of the density of the hydrogen bonds, which weaken the self-healing ability. When the length of the PPG blocks is relatively short, the positive effect of the increase of fraction of flexible PPG segments overcomes the negative effect of the decrease of hydrogen bond density, thus leading to the improvement in the self-healing ability of the PU samples. When the length of the PPG blocks is relatively long, the negative effect of the decrease of hydrogen bond density is dominant, thus resulting in the decrease in the self-healing ability of the PU samples.

The effect of the healing temperature on the self-healing behaviors of the PU samples was also investigated. Figure 6

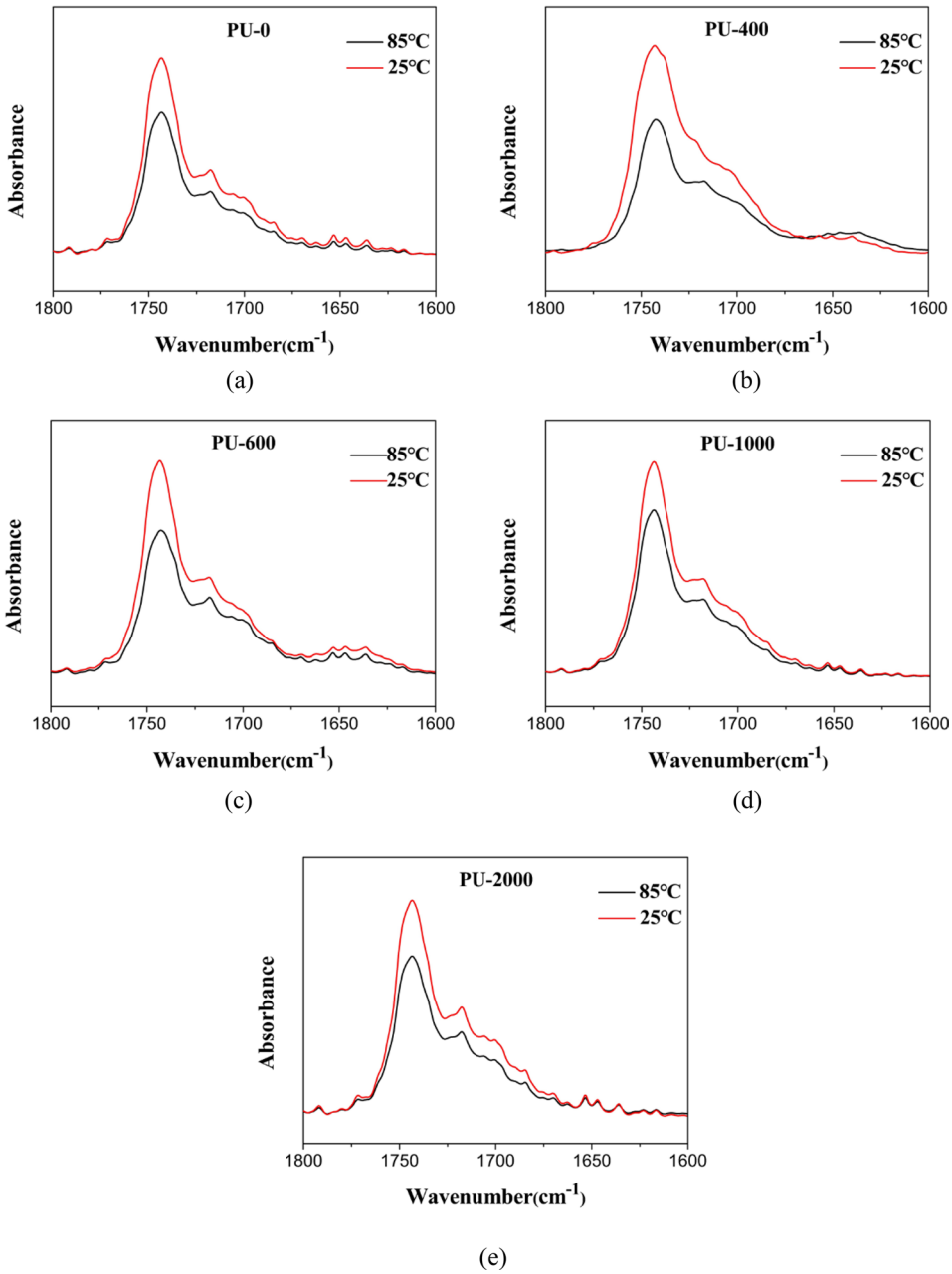

Fig. 7 FTIR spectra of **a** PU-0, **b** PU-400, **c** PU-600, **d** PU-1000 and **e** PU-2000 at 85 °C and 25 °C

displays the stress–strain curves of different original PU samples and these healed for different 1 h at different temperatures, that is, 25 °C, 35 °C, 45 °C, 55 °C and 65 °C, respectively. It can be observed that the tensile strength of the healed PU samples increases with the raise of the healing temperature, demonstrating that the increase of the temperature is beneficial for the self-healing process. The degree of the recovery of the tensile strength for the different PU samples healed at different temperatures is listed in Table 4. The increase of the healing temperature results in the improvement of the recovery degree of the tensile strength. This enhancement in the self-healing ability caused by the increase of the temperature can be owing to the improvement of the chain mobility [28, 44–46]. Previously, our group also found that the temperature increase can lead to the increase of the self-healing ability in ENR filled with ZDMA [28]. In addition, similar to the experimental results of the effect of healing time, compared with the other PU samples, the PU-600 samples also exhibit the highest recovery degree of the tensile strength, namely, the strongest self-healing ability.

Moreover, we try to clarify the mechanisms of the self-healing process in these PU samples containing PPG blocks. As mentioned in the above sections, two factors affect the self-healing process in the PU samples containing PPG block ends: the hydrogen bonds and the

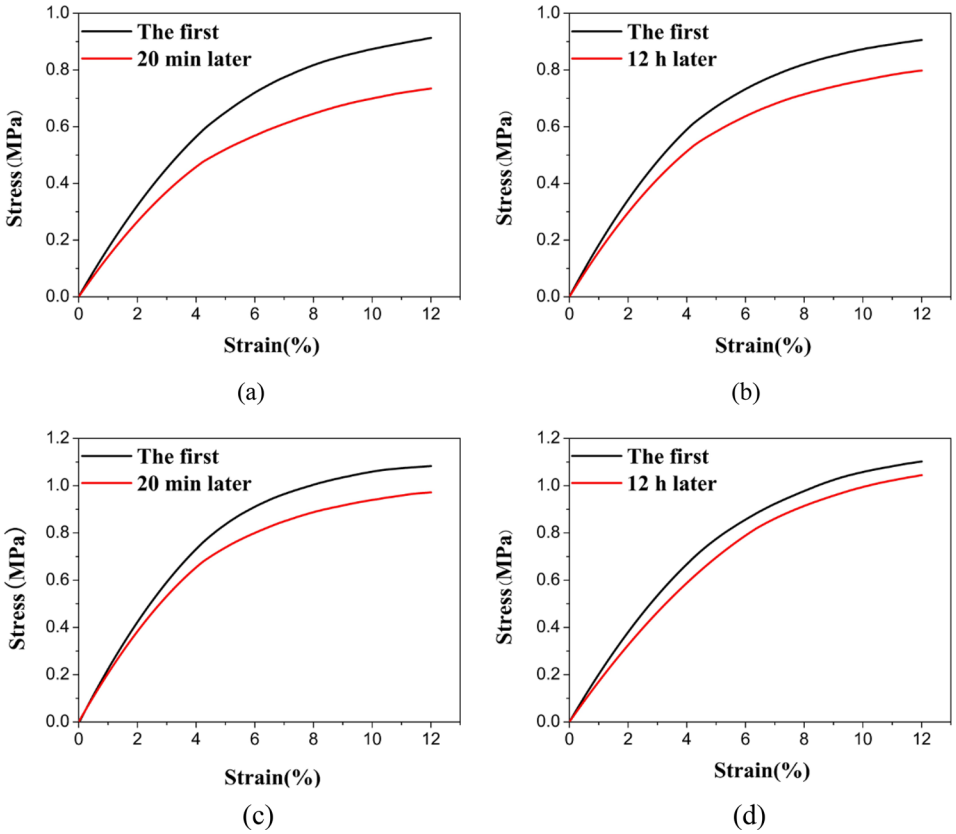

Fig. 8 Stress–strain curves of PU-600 at **a** the first stretching and **b** the second stretching after 20 min and PU-0 at **c** the first stretching and **d** the second stretching after 12 h

high chain mobility of PPG segments. Then, we need to confirm the presence of the hydrogen bonds in the current PU samples. Figure 7 displays the FTIR spectra of different PU samples at different temperatures. Interestingly, as shown in Fig. 7, the FTIR spectra at the low temperature exhibit strong peaks at 1737 cm^{-1}, which can be attributed to C=O in carbonate and urethane groups [31–33]. However, the corresponding peaks in the FTIR spectra at the high temperature become much weaker compared with these at the low temperature, indicating that the hydrogen bonds existing at low temperature are destroyed due to the increase of the temperature [22]. In short, the reduction of the peak intensity corresponding to the damage of hydrogen bonds caused by the temperature increase demonstrates the presence of the hydrogen bonds in the PU samples.

Furthermore, consecutive tensile tests were applied to reveal the effect of hydrogen bonds on the recovery of tensile strength. As shown in Fig. 8, it can be found that for both the PU samples (PU-600 and PU-0) the stress at the strain of 12% during the first stretching is higher than that during the second stretching after 20 min and 12 h. Table 5 further shows that the stress at the strain of 12% during the second stretching after 12 h is higher than that after 20 min, demonstrating that the longer time interval can lead to the better recovery of mechanical properties in the PU samples. During the first stretching, some hydrogen bonds would break. Then, during the subsequent second stretching, the corresponding stress will be lower than that during the first stretching, since fewer hydrogen bonds can contribute to stress. However, if the interval between the two consecutive tensile tests is higher, more hydrogen bonds will reform, thus leading to the higher stress [22, 41]. Accordingly, the reformation of the hydrogen bonds indeed can cause the recovery of mechanical properties.

Table 5 The ratio of the stress at strain of 12% during the first stretching to that during the second stretching

Stress (MPa)	20 min later (%)	12 h later (%)
PU-0	89.71	94.75
PU-400	83.28	90.72
PU-600	80.44	88.09
PU-1000	76.84	83.14
PU-2000	75.67	80.13

4 Conclusion

In summary, this work provides a strategy and mechanism to prepare traditional PU materials with excellent self-healing properties. This strategy depends on the strong mobility of the flexible PPG blocks at the ends of the PU chains and the reversible hydrogen bonds forming between urethane carbonyl groups or carbonyl groups in PCDL segments and urethane NH groups. The soft blocks at the ends of the PU chains have strong fluidity, which is conducive to the chain diffusion and self-healing process around the damage area. In addition, the amino groups form hydrogen bonds with the carbonyl groups, which can further ensure the effective healing of the fractures in the PU materials. We take the PU-600 sample as a typical representative of this strategy. Its tensile strength reaches 20.1 MPa. After complete fracture, the healing rate can reach 79.85% at 45 °C for 2 h and 82.54% at 65 °C for 1 h. Its comprehensive performance is superior to the other self-healing PUs.

It is worth noting that the aim of this work is to synthesize self-healing PU materials with excellent self-healing property by using common monomers and reasonable molecular design. In other words, this strategy provides a way to endow traditional PU materials with self-healing properties, a powerful reference to simplify the synthesis method and production process of self-healing PU materials and a convenience for large-scale production and application of self-healing PU materials.

Acknowledgements This work was financially supported by National Natural Science Foundation of China (No. 21404050). Hao also thanks the supports from Postdoctoral Science Foundation of China (No. 2019M651478), Natural Science Foundation of Jiangsu Province (No. BK20190866) and Natural Science Foundation of the Higher Education Institutions of Jiangsu Province (No. 18KJB150009).

References

1. P. Cordier, F. Tournilhac, C. Soulieziakovic, L. Leibler, Nature **451**, 977–980 (2008)
2. V.K. Thakur, M.R. Kessler, Polymer **69**, 369–383 (2015)
3. J. Dahlke, S. Zechel, M.D. Hager, U.S. Schubert, Adv. Mater. Interfaces **5**, 1800051 (2018)
4. J. Wu, L.H. Cai, D.A. Weitz, Adv. Mater. **29**, 1702616 (2017)
5. H. Wang, H. Liu, Z. Cao, W. Li, X. Huang, Y. Zhu, F. Ling, H. Xu, Q. Wu, Y. Peng, B. Yang, R. Zhang, O. Kessler, G. Huang, J. Wu, Proc. Natl. Acad. Sci. USA **117**, 11299–11305 (2020)
6. L. Liu, L. Zhu, L. Zhang, Macromol. Chem. Phys. **219**, 1700409 (2018)
7. J. Liu, J. Liu, S. Wang, J. Huang, S. Wu, Z. Tang, B. Guo, L. Zhang, J. Mater. Chem. A **5**, 25660–25671 (2017)
8. Q. Zhang, S. Niu, L. Wang, J. Lopez, S. Chen, Y. Cai, R. Du, Y. Liu, J. Lai, L. Liu, C. Li, X. Yan, C. Liu, J.B.H. Tok, X. Jia, Z. Bao, Adv. Mater. **30**, 1801435 (2018)
9. Y. Liu, Q. Zhou, Y. Nie, Z. Zhou, Z. Liang, J. Inorg. Organomet. Polym. **30**, 337–348 (2020)
10. Y. Liu, Y. Wei, R. Liu, Z. Liang, J. Yang, R. Zhang, Z. Zhou, Y. Nie, J. Inorg. Organomet. Polym. **30**, 1553–1565 (2020)
11. Y. Wei, H. Wu, G. Weng, Y. Zhang, X. Cao, Z. Gu, Y. Liu, R. Liu, Z. Zhou, Y. Nie, J. Polym. Res. **25**, 173 (2018)
12. Y. Nie, Z. Gu, Y. Wei, T. Hao, Z. Zhou, Polym. J. **49**, 309–317 (2017)
13. Y. Nie, J. Polym. Res. **22**, 1 (2015)
14. N. Hannewald, M. Enke, I. Nischang, S. Zechel, M.D. Hager, U.S. Schubert, J. Inorg. Organomet. Polym. **30**, 230–242 (2020)
15. J. Brassinne, C. Fustin, J. Gohy, J. Inorg. Organomet. Polym. **23**, 24–40 (2013)
16. Z.S. Petrović, J. Ferguson, Prog. Polym. Sci. **16**, 695–836 (1991)
17. D.K. Chattopadhyay, K.V. Raju, Prog. Polym. Sci. **32**, 352–418 (2007)
18. L. Meng, X. Shi, R. Zhang, L. Yan, Z. Liang, Y. Nie, Z. Zhou, T. Hao, J. Appl. Polym. Sci. (2020). https://doi.org/10.1002/app.49314
19. Y. Xu, D. Chen, Macromol. Chem. Phys. **217**, 1191–1196 (2016)
20. Y. Fang, X. Du, Y. Jiang, Z. Du, P. Pan, X. Cheng, H. Wang, ACS Sustain. Chem. Eng. **6**, 14490–14500 (2018)
21. Y. Lin, G. Li, J. Mater. Chem. B **2**, 6878–6885 (2014)
22. Y. Song, Y. Liu, T. Qi, G. Li, Angew. Chem. Int. Ed. **57**, 13838–13842 (2018)
23. H. Daemi, S. Rajabi-Zeleti, H. Sardon, M. Barikani, A. Khademhosseini, H. Baharvand, Biomaterials **84**, 54–63 (2016)
24. Z. Wang, C. Xie, C. Yu, G. Fei, Z. Wang, H. Xia, Macromol. Rapid Commun. **39**, 1700678 (2018)
25. L. Feng, Z. Yu, Y. Bian, J. Lu, X. Shi, C. Chai, Polymer **124**, 48–59 (2017)
26. L. Zhang, Z. Liu, X. Wu, Q. Guan, S. Chen, L. Sun, Y. Guo, S. Wang, J. Song, E.M. Jeffries, C. He, F.L. Qing, X. Bao, Z. You, Adv. Mater. **31**, 1901402 (2019)
27. K. Yu, A. Xin, H. Du, Y. Li, Q. Wang, NPG Asia Mater. **11**, 7 (2019)
28. Y. Liu, Z. Li, R. Liu, Z. Liang, J. Yang, R. Zhang, Z. Zhou, Y. Nie, Ind. Eng. Chem. Res. **58**, 14848–14858 (2019)
29. X. Wu, J. Wang, J. Huang, S. Yang, J. Colloid Interface Sci. **559**, 152–161 (2020)
30. Y. Lai, X. Kuang, P. Zhu, M. Huang, X. Dong, D. Wang, Adv. Mater. **30**, e1802556 (2018)
31. G. Trovati, E.A. Sanches, S.C. Neto, Y.P. Mascarenhas, G.O. Chierice, J. Appl. Polym. Sci. **115**, 263–268 (2010)
32. J.T. Garrett, R. Xu, J. Cho, J. Runt, J.T. Garrett, Polymer **44**, 2711–2719 (2003)
33. X. Chen, L. Huo, C. Jiao, S. Li, J. Anal. Appl. Pyrol. **100**, 186–191 (2013)
34. B. Wu, Z. Liu, Y. Lei, Y. Wang, Q. Liu, A. Yuan, Y. Zhao, X. Zhang, J. Lei, Polymer **186**, 122003 (2019)
35. J. Liu, Q. Liu, X. Zheng, R. Liu, Q. Mu, X. Liu, Polym. Bull. **73**, 647–659 (2016)
36. X. Wang, Y. Fu, P. Guo, L. Ren, H. Wang, T. Qiang, J. Appl. Polym. Sci. **130**, 2671–2679 (2013)
37. P. Pawłowski, G. Rokicki, Polymer **45**, 3125–3137 (2004)
38. A. Prabhakar, D.K. Chattopadhyay, B. Jagadeesh, K.V.S.N. Rsju, J. Polym. Sci. Part A: Polym. Chem. **43**, 1196–1209 (2005)
39. W.B. Hu, *Polymer Physics a Molecular Approach* (Springer, Vienna, 2013)

40. B. Ghobadi Jola, B. Shirkavand Hadavand, K. Didehban, A. Mirshokraie, J. Inorg. Organomet. Polym. **28**, 92–101 (2018)
41. M.C. Luo, J. Zeng, Z.T. Xie, L.Y. Wei, G. Huang, J. Wu, Polymer **105**, 221–226 (2016)
42. G.P. Johari, A. Hallbrucker, E. Mayer, J. Polym. Sci. Part B: Polym. Phys. **26**, 1923–1930 (1988)
43. J. Bao, G. Shi, C. Tao, C. Wang, C. Zhu, L. Cheng, G. Qian, C. Chen, J. Power Sources **389**, 84–92 (2018)
44. S. Schäfer, G. Kickelbick, Polymer **69**, 357–368 (2015)
45. Y. Yang, M.W. Urban, Chem. Soc. Rev. **42**, 7446–7467 (2013)
46. R. Du, Z. Xu, C. Zhu, Y. Jiang, H. Yan, H. Wu, O. Vardoulis, Y. Cai, X. Zhu, Z. Bao, Q. Zhang, X. Jia, Adv. Funct. Mater. **30**, 1907139 (2020)